Effect of contour process parameters on the surface roughness of laser powder bed fusion manufactured 304 stainless steel

Tafadzwa Mashayamombe[1*], *Xola* Madyibi[2], and *Stephen* Matope[3]

[1-3]Department of Industrial Engineering, Stellenbosch University, South Africa

Abstract. Surface roughness remains a major drawback in metal additive manufacturing (AM) processes. Even though finishing operations are applied, the surface roughness is still of interest because additive manufacturing is mainly applied in expensive materials and, in some cases, hard-to-machine materials. Additionally, conventional finishing operations are not viable for intricate components like fine porous structures or cavities, which make AM attractive. Therefore, improving the surface quality of parts created through laser powder bed fusion (LPBF) requires direct optimisation during manufacturing. In this study, the authors investigated the effect of contour process parameters on the surface roughness of vertical surfaces and sloped surfaces associated with up and down surfaces fabricated by LPBF using 304 stainless steel (304 SS) powder feedstock. The study explored the impact of varying laser power and scanning speed separately while holding other parameters constant. The obtained results showed that increasing the speed decreases the surface roughness on the vertical surfaces whereas there was no clear dependency of the roughness on the laser power. The sloped surface consistently exhibited higher roughness on the down skin than the up skin, which can be attributed to deeper laser penetration. Additionally, printed samples indicated reductions in clearance from the CAD model, attributed to unmolten powder particles adhering to the surface. Understanding and optimising surface finish and dimensional accuracy could further accelerate the adoption of LPBF technology in fabricating net-shaped direct-to-service components.

1 Introduction

In recent times, AM has attracted considerable interest, and its adoption to complement conventional manufacturing processes is highly favoured owing to its capacity to fabricate relatively complex components while maintaining structural integrity, enhancing production efficiency, and cutting down expenses [1]. Among the different AM processes available, LPBF stands out as the most popular technique [2]. The LPBF procedure relies on depositing a metal powder layer onto a platform and using a laser to melt a specific slice pattern from the CAD file onto the layer beneath it. This process is repeated layer by layer until the final component is fully produced [3,4]. Apart from the benefits mentioned above, the LPBF

* Corresponding author: 27275396@sun.ac.za

process provides greater material flexibility as different powder feedstock can be blended to achieve the desired performance in the finished part. It also allows the fabricating of almost fully dense or porous metallic parts, as desired, with a precision of dozens of microns [5]. Furthermore, LPBF can print features with a consistent grain structure due to the continual heating and cooling during deposition [6]. Due to these factors, LPBF has been well applied in several important fields, such as medicine, aerospace, and energy where it has been explored with metal alloys and other high-performance metals [7,8].

Even though the LPBF technique offers many advantages over traditional production methods, it also introduces its unique problems. Some of these issues are related to the dimensional precision and surface roughness of the as-built parts produced using this technology [9]. It is estimated that more than 130 factors can influence the properties of a part produced using LPBF technology, which can be categorized into machine-related, material-related, process, and post-treatment parameters [10]. The surface roughness of the printed components is also impacted by these parameters, the volumetric energy density (VED) of the contour parameters, and the slope angle of the part, with roughness typically being lower on the up skin compared to the down skin [11]. Wang et al. [5] investigated the characteristics of features manufactured by LPBF using 316 stainless steel. They created a 3D model with various features and different types of corners. Their study suggested that the optical spot diameter determines the dimensional accuracy of thin walls. They recommended contour scanning to account for the discrepancy between the actual melting area and the component's cross-sectional area, as they noted that part scanning resulted in larger manufactured wall sizes compared to the design. This would effectively influence the surface roughness of the printed part. Wang et al. [5] also noted that when using powder as support for overhanging structures, the molten pool can seep into the surrounding powder, leading to powder adherence. This also influences the surface roughness of the final part, and its effect varies according to the part's angle of inclination relative to the base plate.

Vu et al. [11] investigated surface roughness, examining stainless steel 316L specimens produced by two identical manufacturing systems in different locations using LPBF technology. This study examined walls of various thicknesses and different angles of inclination measured relative to the building direction, as illustrated in Fig. 1. This study concluded that wall thickness did not have a notable effect on surface roughness. However, the inclination angle significantly influenced surface roughness, particularly on down skin areas, leading to rougher surfaces at higher angles for both machines in different locations. Specimens inclined at a 45° angle were found to display surface roughness values higher than those of vertical specimens.

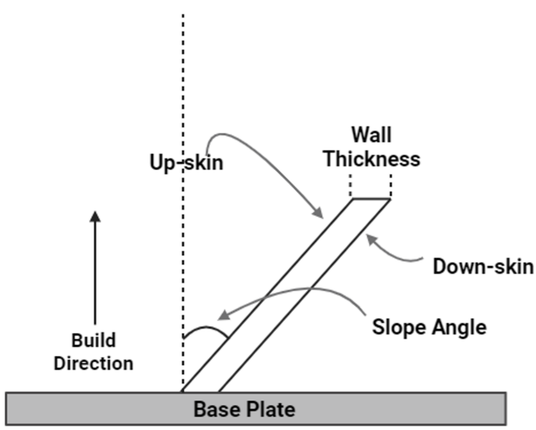

Fig. 1. Schematic image of specimen thickness and slope angle as illustrated by Vu *et al.* [11].

Vu *et al.* [12] examined the surface roughness of 316L wall structure specimens in another related study. These specimens had differing wall thicknesses and slope angles and were produced using different powder feedstock and manufacturing systems. This study found minor differences in surface characteristics among the different systems. It revealed significant dependencies of mean peak-to-valley height (Rz) and arithmetic mean roughness (Ra) on the slope angle across different manufacturing systems, with notable differences in roughness values between the down skin and up skin. Higher roughness values were observed in the down skin, attributed to more randomly attached powder material because of deeper laser penetration. The study suggested that the effect of wall thickness on Rz and Ra was negligible within the range of 1.5 mm to 5 mm used in the study.

A considerable number of publications have been released investigating the surface roughness of metal LPBF. These studies have highlighted the use of build process parameters for contour scanning and part scanning. However, only 30% of the 83 articles reviewed by Obilanade [13] in 2021, in a literature review focusing on different aspects of surface roughness of components produced with metal LPBF, were on stainless steel. Most of the available articles which looked at stainless steel focused on 316L. It is the authors' understanding that there is a limited investigation on the surface characterisation of 304 SS. Hence, the current study focuses on the surface roughness characterisation on vertical and sloped surfaces of 304 SS samples fabricated by reducing the energy density of contour parameters by increasing the scanning speed, as proposed by Liu *et al.* [14], and reducing laser power. Each process parameter was examined separately while keeping the other parameters constant. This investigation aims to understand how contour scanning energy density and each specific parameter influence surface roughness in LPBF-produced parts.

2 Materials and methods

Fig. 2 below shows a flow diagram of the research conducted in this study. The highlighted investigations constitute the stages in the study's methodology.

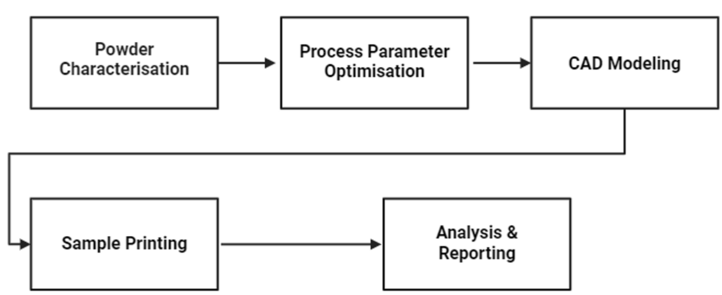

Fig. 2. Methodology flow diagram.

2.1 Powder feedstock

The 304 SS powder used in this study was sourced from AVIMETAL AM. The chemical composition of this powder is given in Table 1, as provided by the supplier. Further analysis was conducted on the virgin powder used in this study. The particle size distribution (PSD) analysis conducted by the authors indicated that the PSD of this feedstock was within the typical range recommended for LPBF powders, with D_{10} of 17.4 µm, D_{50} of 30.2 µm, and D_{90} of 50.9 µm.

Table 1: Chemical composition of 304SS powder feedstock.

Element	**Fe**	**Cr**	**Ni**	**Mn**	**Si**	**P**	**C**	**S**	**O**	**N**
Composition (wt. %)	Bal	18.62	10.50	1.12	0.20	0.01	0.01	0.005	0.077	0.105

Scanning electron microscopy (SEM) analysis was also performed on the feedstock. The powder particles exhibited a spherical particulate morphology with smooth surfaces, as shown in Fig. 3b. However, it can be observed that some of the particles are stuck together. This could have resulted from the manufacturing processes used to produce the powders [15]. The PSD in Fig. 3a indicates that the powder feedstock had a high content of fine particles as it is positively skewed. Such powders are reported to yield high part densities and favourable scan surfaces [16,17].

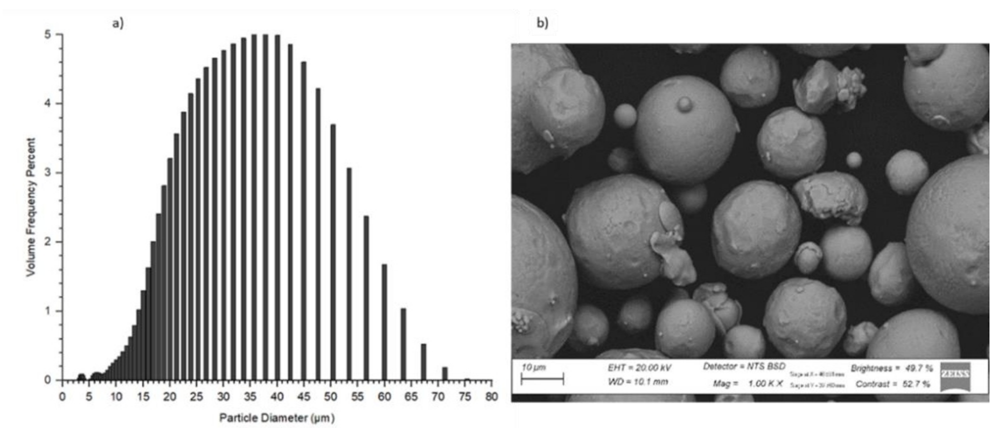

Fig. 3. a) Volume frequency percentage of the powder b) SEM image of the powder.

2.2 CAD models and LPBF printing

The CAD models used in this study were created using the SolidWorks software. These models had a clearance of 0.2 mm between vertical surfaces and 0.4 mm between surfaces slanting at 45° from the build plate. These clearances are illustrated in the CAD models in Fig. 4, and they refer to the distance left in-between two adjacent LPBF printed surfaces. The decision to use a 45° angle was based on the fact that this is the recommended angle for self-support [18] whereas the CAD clearances were used to test the dimensional accuracy of the LPBF technology. The printing was performed on a GE Additive Concept Laser Mlab 200R LPBF machine, ideally suited for high surface quality and creating the finest part structures. Only a single contour was scanned in this study, offset at 0.0675 mm. The process parameters used for part scanning are shown in Table 2. These parameters were proven to achieve a relative density of 99.72% in another related study by the authors. These parameters were used with an island scanning strategy. The successive layers of the print were rotated by 90°, and the hatching had an overlap distance of 0.0525 mm.

Table 2. Build parameters.

Process Parameter	Value
Laser Power	200 W
Scanning Speed	1500 mm/s
Hatch Spacing	0.05 mm
Layer Thickness	30 μm

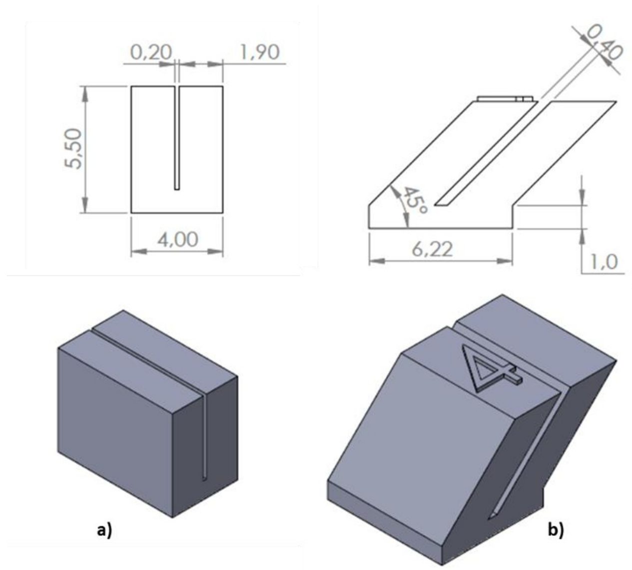

Fig. 4. a) Vertical and b) Slanting CAD models of samples investigated in the study.

The printing parameters for the contour surfaces were varied, specifically the scanning speed and laser power, to investigate the effect of these two parameters on surface roughness. Sixteen samples were printed on the same build in this study. Of these 16 samples, 8 were vertical, and the other 8 were slanted at an angle of 45 degrees. Where the processing parameters were varied for contour printing, a constant factor of 250 mm/s increased the scanning speed, and the laser power was reduced by a constant factor of 20 W. Hatch spacing was kept constant at 0.05 mm in these investigations. Table 3 shows the different parameters used to print the contour surfaces to understand better the impact of scanning speed and laser power on surface finish. Parameter 7 was obtained by considering the average for the two ranges of laser power and scan speed. Table 3 presents the pairing of the samples and process parameters used to print them. The bulk of each part was printed using the parameters listed in Table 2. The CAD drawings for the vertical and slanting samples printed in this work are shown in Fig. 4.

Table 3. Contour printing parameters.

Sample	Laser Power (W)	Scanning Speed (mm/s)
S1, AS1	200	1750
S2, AS2	200	2000
S3,AS3	200	2250
P1, AP1	180	1500
P2, AP2	160	1500
P3,AP3	140	1500
S, P, AS, AP	160	2000

The samples were categorised into two groups based on whether the variation was in speed or power.

- Samples S1, S2, and S3 are the vertical samples where only the speed was varied (increased) while keeping the power constant. The variations in speed are represented by S1, S2, and S3, with each designation corresponding to a different speed setting.
- Samples P1, P2, and P3 are the vertical samples where only the power was varied (decreased) while keeping the speed constant. The variations in power are represented by P1, P2, and P3, with each designation corresponding to a different power setting.

For the slanted samples, the prefix "A" was used to distinguish them from the vertical ones:

- Samples AS1, AS2, and AS3 are the slanted samples corresponding to the vertical samples S1, S2, and S3 speed variations. Thus, AS1, AS2, and AS3 reflect the impact of varying speed on slanted samples.
- Samples AP1, AP2, and AP3: These are the slanted samples corresponding to the power variations of the vertical samples P1, P2, and P3. Thus, AP1, AP2, and AP3 reflect the impact of varying power on slanted samples.

2.3 Surface roughness measurements

Surface roughness measurements were taken using a Mahr MarSurf PS 10 profilometer. The instrument was verified using a specimen with a predetermined Rz value of 9.55 µm. A reading of 9.316 µm was obtained, within 10% of the actual value. This verification confirmed that the instrument was performing within acceptable limits and could be reliably used for the surface roughness measurement exercise. The profilometer was set to travel 1.5 mm over the surface of the sample to determine the Ra and Rz of the LPBF printed samples. Seven measurements were conducted at different locations on the sample, recording Ra and Rz values each time. These measurements were randomised in terms of location and direction to minimise any potential bias related to specific orientations or locations. The average of the seven Ra measurements was calculated to obtain the final Ra value, and the same exercise was done for the Rz measurements to obtain the final Rz value for the sample.

3 Results and discussions

All the samples in this investigation were printed successfully. The resultant clearances after printing were measured by means of a feeler gauge to determine the AM process's dimensional accuracy and investigate the effects of varying the two studied parameters, laser power and scan speed, on the final printed part. The clearance measurement results were consistent for all the samples. The vertical surfaces had a resultant clearance of 0.1mm, whereas the sloped surfaces had a resultant clearance of 0.2 mm. This is one of the limitations of LPBF, which was reported by Wang et al. [5] that the actual melting area is always larger than the designed size. Other studies have also indicated that the clearances that result from LPBF are always less than the intended clearances from the design [19,20].

Fig. 5 gives the surface roughness results for the vertical surfaces. Increasing the speed of the contour parameters showed a consistent correlation with both the Ra and Rz values of the vertical surfaces of the sample, where a sharp drop was recorded at first, which was then followed by a gradual decrease in the surface roughness, as shown in Fig. 5a. The trend obtained by increasing the speed was interrupted after the power was changed for Rz while it was maintained for Ra. Hence, it can be concluded that increasing the scanning speed results in an improved surface finish of the vertical walls of the sample. Increasing the speed of the laser resulted in a reduced VED per unit area. This could have led to a more uniform surface since the heat-affected zone was reduced, and, hence, fewer surrounding powder particles were attached to the surfaces of the samples [5]. Reducing the laser power, on the other hand, might have led to insufficient energy to melt the powder consistently fully, resulting in incomplete fusion and effectively increasing the surface roughness. Regardless of the sharp drop in the surface roughness at first, decreasing the power did not show any clear dependency of the Ra and Rz values of the surface roughness, as seen in Fig. 5b.

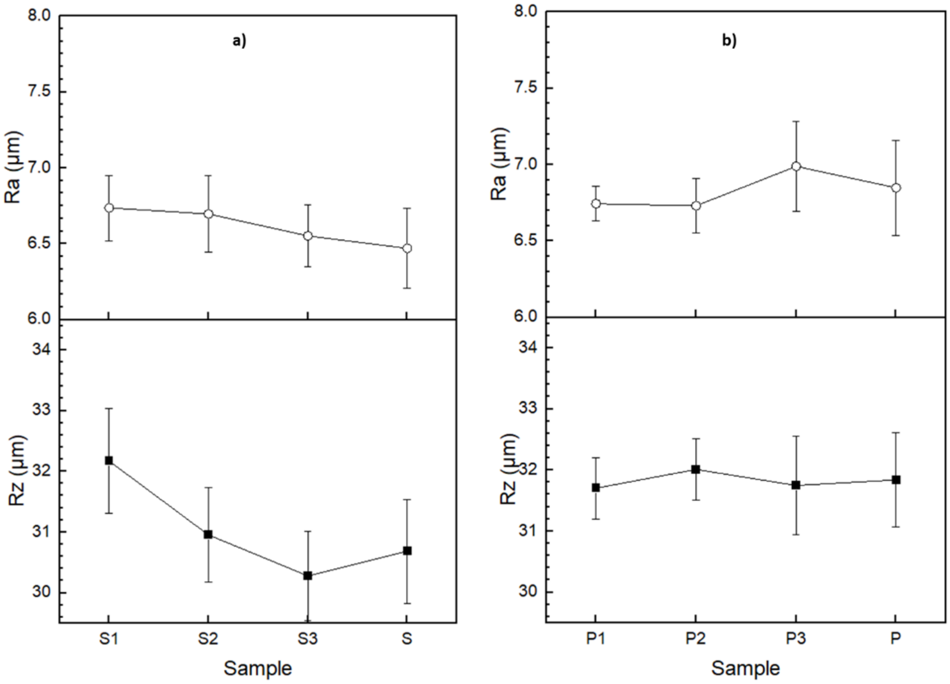

Fig. 5. Effect of a) scan speed and b) laser power on vertical surfaces.

Analysis of the up skin surface showed that both the Ra and Rz values of surface roughness increase with an increase in contour scanning speed on the up skin, as shown in Fig. 6. The two also show a decrease when the average laser power and scanning speed are used. Vu et. al [12] reported that the surface roughness of the up skin is dominantly influenced by the staircase effect in relation to the layer thickness. The uniform surface finish that was observed to be improving with an increase in scanning speed could have resulted in the staircase effect being more pronounced in the up skin of the sloped samples and, hence, the increase in the surface roughness. As with the vertical walls, the Ra and Rz values still showed no clear dependency on the power. However, these values were almost consistent in the same range.

The suffixes "u" and "d" were used to indicate that reading had been taken on the up and down skin, respectively. The Ra and Rz values also showed a consistent trend with increased speed on the down skin. At first, there was a slight increase in both values, then a sharp decrease as the speed was further increased, as shown in Fig. 7. A decrease in laser power, on the other hand, showed an opposite effect where both the Ra and Rz values first dropped, and then there was a sharp increase. As expected, the Ra and Rz values are greater on the down skin. This can be explained in terms of the laser penetration depth and heat dissipation in the exposed powder bed. On the top surface, the heat can radiate upwards, but on the down skin, heat can only transfer downwards into the limited mass of previously deposited material. This limited heat dissipation leads to incomplete melting and a rougher surface due to a higher laser penetration depth [12]The slope angle also has a more pronounced effect on the down skin than on the up skin. The increase in surface roughness is, therefore, due to an increase in the amount of randomly attached powder material on the hanging surface, as there is a higher tendency for loose powder underneath the layer being melted to partially fuse and adhere to the surface, resulting in higher roughness.

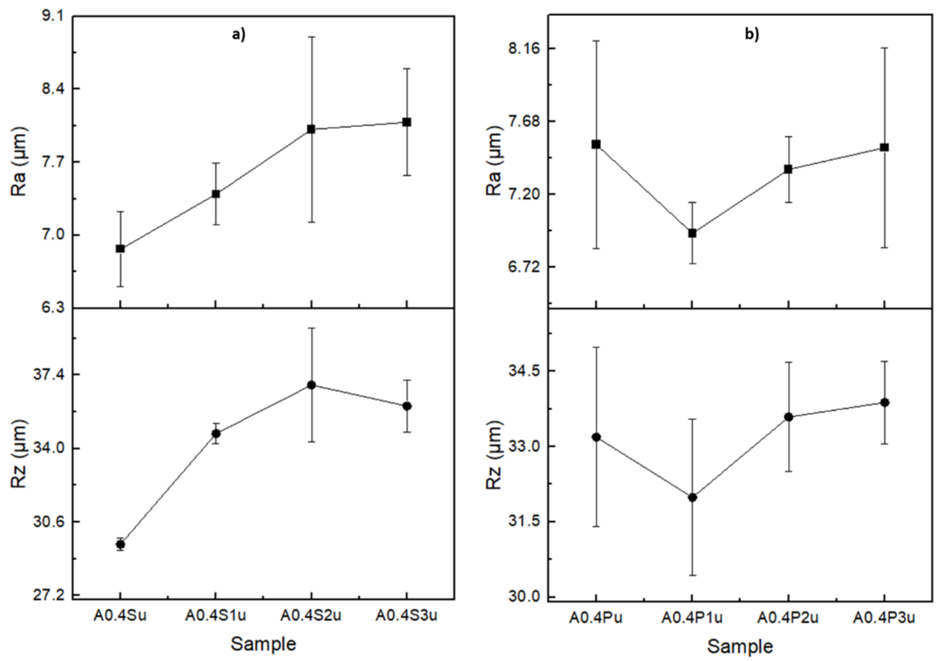

Fig. 6. Effect of a) scan speed and b) laser power on the up skin.

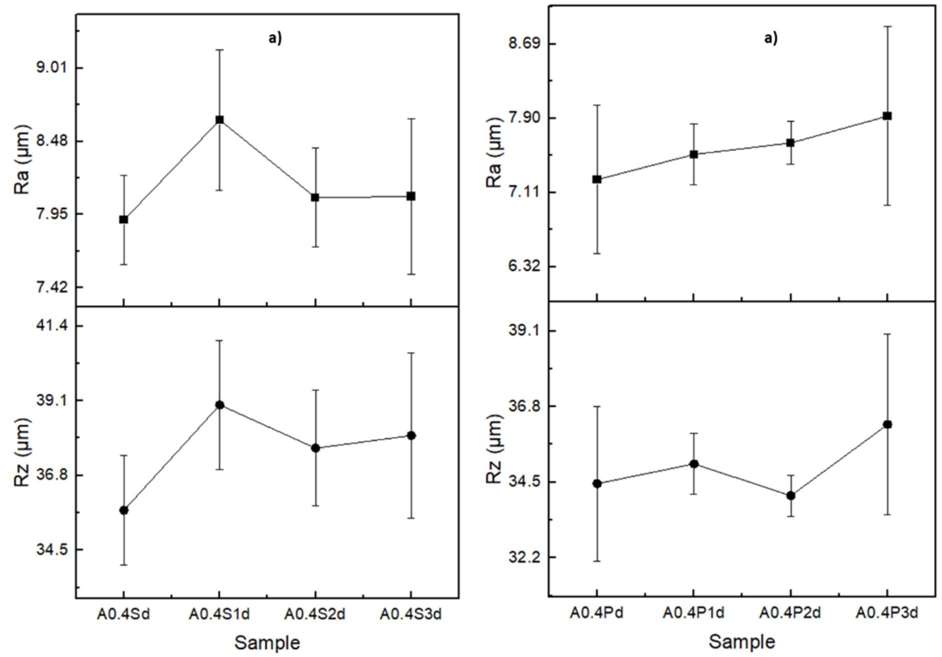

Fig. 7. Effect of a) scan speed and b) laser power on the down skin.

4 Conclusion

An analysis of the effect of the contour process parameters, particularly the laser power and scanning speed, has been presented to further the understanding of the resultant surface roughness and the clearances in 304 SS printed samples. The resultant clearances highlighted one of the limitations of LPBF, which is achieving precise dimensional accuracy. On vertical surfaces, increasing scan speed led to a more uniform surface finish due to reduced energy density, resulting in smoother surfaces. On the other hand, decreasing the laser power did not clearly affect the surface roughness. Therefore, only scanning speed showed a great influence on the surface quality of the vertical surfaces. Analysis of up skin and down skin surfaces also revealed distinct trends, which can be attributed to the staircase effect and laser penetration depth, respectively. Overall, while the differences in surface roughness were within micron ranges, the insights of this study are of significant implications, particularly for applications requiring high precision and smooth surface finish. Future work could look at further qualitative analysis and characterisation of the of the individual features contributing to surface roughness using advanced technologies like scanning electron microscope. The current study used a single contour, other studies could also investigate the effect of having several contour scans.

Author[1] was enrolled for an MEng. (Research) Industrial Engineering degree in the Department of Industrial Engineering, Stellenbosch University. The authors declare that they have no known competing financial interests or personal relationships that could have appeared to influence the work reported in this paper. The Intra-Africa Academic Mobility Scheme of the European Union is acknowledged for the funding under the Education for Laser-based Manufacturing sponsorship.

References

1. M. Ghayoor, K. Lee, Y. He, C. Hung Chang, B. K. Paul, and S. Pasebani, Addit Manuf **32**, (2020)
2. Y. Yao, L. Fan, R. Ding, C. Franke, Z. Yang, W. Liu, T. Li, and H. Chen, J Mater Sci Technol **184**, 180 (2024)
3. D. Dev Singh, T. Mahender, and A. Raji Reddy, in *Mater Today Proc* (Elsevier Ltd, 2021), pp. 350–355
4. J. C. Fox, S. P. Moylan, and B. M. Lane, in *Procedia CIRP* (Elsevier B.V., 2016), pp. 131–134
5. D. Wang, S. Wu, Y. Bai, H. Lin, Y. Yang, and C. Song, J Laser Appl **29**, (2017)
6. N. Jeyaprakash, C. H. Yang, and K. R. Ramkumar, Metals and Materials International **27**, 5179 (2021)
7. Y. Ma, Y. Gao, L. Zhao, H. Zhang, D. Li, L. Yang, and C. Yu, Materials **16**, (2023)
8. S. Zhang, S. Wang, X. Feng, Z. Ning, J. Hou, and W. Kuang, Acta Mater **244**, (2023)
9. M. Galati, P. Minetola, and G. Rizza, Materials **12**, (2019)
10. I. Yadroitsev, I. Yadroitsava, A. Du Plessis, and E. MacDonald, *Fundamentals of Laser Powder Bed Fusion of Metals*, 1st Edition (Elsevier, 2021)
11. H. M. Vu, S. Meiniger, B. Ringel, H. C. Hoche, M. Oechsner, M. Weigold, M. Schmitt, and G. Schlick, Metals (Basel) **12**, (2022)
12. H. M. Vu, S. Meiniger, B. Ringel, H. Hoche, M. Oechsner, M. Weigold, and C. Seidel, Progress in Additive Manufacturing (2024)
13. D. Obilanade, C. Dordlofva, and P. Törlind, in *Proceedings of the Design Society* (Cambridge University Press, 2021), pp. 2841–2850
14. Y. Liu, Y. Yang, X. Yang, D. Wang, and Z. Xiao, in *Proceedings of the International Conference on Progress in Additive Manufacturing* (Pro-AM, 2014), pp. 346–351
15. E. J. Garboczi and N. Hrabe, Addit Manuf **31**, (2020)
16. A. B. Spierings, N. Herres, and G. Levy, Rapid Prototyp J **17**, 195 (2011)
17. B. Liu, R. Wildman, C. Tuck, I. Ashcroft, and R. Hague, *Investigation the Effect of Particle Size Distribution on Process Parameters Optimization in Selective Laser Melting Process* (2011)
18. H. Hassanin, L. Finet, S. C. Cox, P. Jamshidi, L. M. Grover, D. E. T. Shepherd, O. Addison, and M. M. Attallah, Addit Manuf **20**, 144 (2018)
19. C. P. Jiang, A. T. Wibisono, S. H. Wang, T. Pasang, and M. Ramezani, Metals (Basel) **12**, (2022)
20. Y. Liu, J. Zhang, Y. Yang, J. Li, and J. Chen, J Manuf Process **27**, 98 (2017)